PREDICTING THE DIVERSION LENGTH OF CAPILLARY BARRIERS USING STEADY STATE AND TRANSIENT STATE NUMERICAL MODELING: CASE STUDY OF THE SAINT-TITE-DES-CAPS LANDFILL FINAL COVER

Benoit Lacroix Vachon[1], Amir M. Abdolahzadeh[2], and Alexandre R. Cabral[3*]

Lacroix Vachon, B., Abdolahzadeh, A.M. and Cabral, A.R. (2015). Predicting the diversion length of capillary barriers using steady state and transient state numerical modeling: Case study of the Saint-Tite-des-Caps landfill final cover. Canadian Geotech. J. 52: 2141–2148 (2015) dx.doi.org/10.1139/cgj-2014-0353

Abstract:

Covers with capillary barrier effect (CCBE) have already been proposed to meet regulatory requirements for landfill final covers. Modeling of CCBE may be a relatively complex and time consuming task. Simpler, albeit conservative, design tools – such as steady state numerical analyses – can be, in certain cases, justifiable and have a positive impact in the practice. In this study, we performed numerical simulations of the experimental CCBE constructed on the Saint-Tite-des-Caps landfill (Quebec). The CCBE consists of a capillary barrier, composed of sand and gravel, on top of which a layer of deinking by-products (DBP) was installed as a protective layer (also to control seepage). The addition of a protective layer over the infiltration control layer (such as a capillary barrier) is required nearly everywhere. In many European countries, such as Germany and the Netherlands, a thick "recultivation" layer is required. The results of numerical simulations were compared to the *in situ* behaviour of the Saint-Tite CCBE as well as to analytical solutions. The effectiveness of the capillary barrier was assessed by quantifying the diversion length (DL), which reflects the lateral drainage capacity of the CCBE, i.e. the capacity to drain water laterally. The latter, if collected, prevents seepage into the waste mass. This study

[1] P.Eng, M.Sc.A. Groupe Qualitas inc., member of the SNC-LAVALIN group, Montreal, QC, Canada. Formerly with the Department of Civil Engineering, Université de Sherbrooke.
[2] P.Eng., Ph.D. AECOM, Montreal, QC, Canada. Formerly with the Department of Civil Engineering., Université de Sherbrooke.
[3] Department of Civil Engineering, Faculty of Engineering, Université de Sherbrooke, 2500, boul. de l'Université, Sherbrooke, QC J1K 2R1, Canada.
* Corresponding author: A.R. Cabral (Alexandre.Cabral@Usherbrooke.ca).

shows that, when the seepage rate reaching the top layer of the capillary barrier is controlled, it is possible to predict the worst case scenario in terms of seepage (and therefore predict the shortest DL) using steady state numerical simulations. These simpler-to-perform numerical simulations could be adopted, at least in a pre-feasibility study for cases with a similar profile as the one at the Saint-Tite-des-Caps experimental CCBE.

Key words: Landfills, Deinking by-products, Final covers, Alternative cover design.

Résumé :

Des recouvrements avec effet de barrière capillaire (CCBE) ont déjà été proposés pour répondre aux exigences législatives des recouvrements finaux des sites d'enfouissement. La modélisation d'une CCBE est une tâche relativement complexe et qui peut demander du temps. La possibilité d'effectuer des modélisations numériques plus simples, comme les analyses en régime permanent, tout en offrant une solution conservatrice et éprouvée, pourrait avoir un impact positif dans la pratique. Dans la présente étude, des simulations numériques de la CCBE expérimentale installée au site d'enfouissement de Saint-Tite-des-Caps (Québec) ont été réalisées. La CCBE est constituée d'une barrière capillaire, composée de sable et de gravier, au-dessus de laquelle une couche de sous-produits de désencrage (DBP) a été installée. Cette dernière agissait comme couche de protection et de contrôle des infiltrations. L'ajout d'une couche de protection au-dessus de la barrière capillaire est généralement exigé dans les règlements concernant l'enfouissement de matières résiduelles. Dans certains pays européens, dont l'Allemagne et Les Pays-Bas, on exige une couche épaisse dénommée « recultivation layer ». Les résultats des simulations numériques sont comparés au comportement *in situ* de la CCBE ainsi qu’à certaines solutions analytiques. L’efficacité de la barrière capillaire a été évaluée en quantifiant la longueur de transfert (DL), qui reflète la capacité de drainage latérale de la CCBE. L’eau drainée latéralement doit être captée, évitant ainsi sa percolation vers la masse de déchets. La présente étude démontre que, lorsqu’on contrôle le débit de percolation atteignant la couche supérieure de la barrière capillaire, il est possible de prédire le pire scénario d’infiltration (et donc de prédire la DL la plus courte) par le biais de simulations numériques en régime permanent. Ces simulations numériques plus simples à réaliser pourraient être adoptées, du moins dans le cadre d’une étude de préfaisabilité pour des cas ayant un profil semblable à celui du recouvrement final de la plateforme expérimentale de Saint-Tite-des-Caps.

Mots-clés : Lieux d’enfouissement sanitaire, sous-produit de désencrage, barrière capillaire, recouvrement final, recouvrement alternatif.

1 Introduction

Covers with capillary barrier effect (CCBE) have been proposed as an alternative final cover system for mine residues and waste disposal facilities (Stormont, 1996; Barth and Wohnlich, 1999; Morris and Stormont, 1999; von Der Hude et al., 1999; Khire et al., 2000; Bussière et al., 2003; Kämpf et al., 2003; Wawra and Holfelder, 2003; Aubertin et al., 2006). Regulatory requirements in countries such as Germany and the Netherlands include the addition of a thick layer (“recultivation layer”) overlying the capillary barrier (e.g. Giurgea et al., 2003; Hupe et al., 2003) in final covers for solid waste landfills. Relatively fine-textured soils can be employed and therefore become a seepage control layer.

In inclined CCBE, the moisture retaining layer (MRL) diverts (or drains) the rainfall that seeps through the top-most layers of the cover system downslope. The maximum lateral flow the MRL can divert, the diversion capacity (Q_{max}), is attained at a critical zone along the interface called the breakthrough zone. Beyond this zone, capillary forces no longer retain the accumulated water within the MRL; in other words, moisture starts to infiltrate into the capillary break layer (CBL). This transfer of water becomes more accentuated at the diversion length, DL (Ross, 1990), where the downward flow into the CBL (and ultimately into the waste mass) reaches a value equal to the seepage flow rate.

The fundamental design parameters for a CCBE system and the determination of its associated DL are the hydraulic conductivity functions – often derived from the water retention curves (WRC) - of the various layer materials, slope of the cover system, length of the slope, climatic conditions and allowable seepage flow rate. Several authors have discussed how the water storage and lateral diversion capacity of a capillary barrier is affected by factors such as the material properties and thickness, cover configuration, slope of the interface, and climatic conditions (Morris and Stormont, 1998; Zhan et al., 2001; Tami et al., 2004; Parent and Cabral, 2006; Yanful et al., 2006; Aubertin et al., 2009).

Depending on climatic conditions, the amount of precipitation that infiltrates through the surface may exceed the water storage capacity of the MRL and the diversion capacity of the CCBE, thereby limiting lateral drainage within the MRL and hence reducing the diversion length. Abdolahzadeh et al. (2011a; 2011b) suggested adding a seepage control layer on top of the MRL in order to limit the seepage flow rate to a maximum equal to the saturated hydraulic conductivity of the seepage control layer. It needs, nonetheless, to be acknowledged that the maximum flow rate may be dictated by the presence of cracks within the seepage control layer.

In this study, transient state numerical simulations were performed based on the experimental CCBE constructed on the Saint-Tite-des-Caps landfill (Lacroix Vachon et al., 2007; Abdolahzadeh et al., 2008; Abdolahzadeh et al., 2011a; Abdolahzadeh et al., 2011b). The results of the numerical simulations under transient state were compared to the response of the experimental CCBE for a typical year (Abdolahzadeh et al., 2011a; Abdolahzadeh et al., 2011b), to the results obtained by steady state numerical simulations, to the results obtained using a well-known analytical solution (Ross, 1990), and to the results obtained using an adaptation of the latter (Parent and Cabral, 2006).

Transient-state numerical simulations better define the behaviour of a CCBE and therefore constitute a more precise design tool. This is partly attributed to the fact that the precipitation rate changes continuously, thus the seepage flow rate reaching the top of the CCBE and the suctions at the interface between the MRL and CBL change accordingly. As a consequence, it is expected that the diversion length varies continuously and the design process needs to consider these naturally-occurring variations. Despite this fact, the results reported in this paper show that when the seepage flow rate level can be controlled, a steady state analysis can predict the worst-case scenario in terms of diversion length, and can therefore be considered at least for the pre-design (feasibility) phase of a project.

2 Materials and Methods

2.1 Composition of the materials

The longitudinal profile of the 10-m wide and 30-m long experimental cover installed at the Saint-Tite-des-Caps landfill site was presented by Abdolahzadeh et al. (2011a), who describe the instrumentation installed in it. The upper layer, constructed with random fill, protects the lower layers and is required by Quebec landfill regulations. The immediately underlying layer consists of deinking by-products DBP (0.6 m) and forms a hydraulic barrier (or seepage control barrier). The lower part of the experimental final cover includes a capillary barrier made up of a layer of sand (0.4 m) superposed over a layer of gravel (0.2 m).

The water retention curve of DBP (whose Gs = 2.0) was obtained using a pressure plate modified by Parent (2006) to test highly compressible materials (Cabral et al., 2004; Parent et al., 2004; Parent et al., 2007). The experimental results and a fitting curve using the Fredlund and Xing (1994) model are presented in Figure 1. The corresponding Fredlund and Xing (1994) parameters fitting curve and the saturated volumetric water content (θs) value for DBP are presented in Table 1. The porosities (n) of all the materials are equal to their saturated volumetric water contents (θs in Table 1). The WRCs of the sand (Gs=2.65) and gravel (Gs=2.65) were obtained by means of drainage columns (Lacroix Vachon, 2008; Abdolahzadeh et al., 2011a).

The van Genuchten model (1980) was selected as the regression model for the sand and gravel (Figure 1a) and their corresponding van Genuchten parameters are presented in Table 1. Data for the WRC of the waste was taken from the GeoStudio (Geo-Slope Int. Ltd., 2004) database. The main hydraulic properties of the waste, including the van Genuchten (1980) corresponding parameters, are also summarized in Table 1, which also presents the air entry values (ψ_{AEV}) and water entry values (ψ_{WEV}) of most of the different materials employed. These values were determined using the Brooks and Corey (1964) graphical method.

The saturated hydraulic conductivity (k_{sat}) of DBP is equal to 1.0 x 10^{-8} m/s, as obtained by Bédard (2005), Burnotte et al. (2000) and Planchet (2001). The saturated hydraulic conductivity of the sand, 1.5 x 10^{-4} m/s, was estimated using the Hazen (1911) formula, with a cross-check using the neural network in the RETC code (van Genuchten et al., 1991). For the gravel, the k_{sat} (1.5 x 10^{-3} m/s) was also estimated with the Hazen (1911) formula, with a cross-check using the Chapuis (2004) method. The k_{sat} values are presented in Table 1. The *k-fct* of the sand, gravel and waste, shown in Figure 1b, were obtained using the van Genuchten (1980) model, based on the Mualem (1976) formulation.

In the present study, the effect of hysteresis of the WRC was not considered; only the drying curve was used. Zhang et al. (2009) showed that pore water pressure distributions in modeled capillary barriers, as well as the DL location, are influenced by whether or not hysteresis is considered. While it can be important for fine sands, an investigation performed by Maqsoud et al. (2004) showed that for coarse-grained materials, this effect is much less important.

Table 1: Hydraulic properties of the materials used in numerical simulations of the Saint-Tite-des-Caps experimental CCBE.

Figure 1: a) Water retention curve (WRC); and b) *k-fct* of the materials used in numerical simulations.

2.2 Analytical solutions and numerical modeling

2.2.1 Analytical solutions

Various equations can be used to evaluate the DL, such as those proposed by Ross (1990), Steenhuis et al. (1991), Morel-Seytoux (1994) and Walter et al. (2000). Ross (1990) developed analytical relationships for the DL and Q_{max} of a capillary barrier and applied equations based on constant infiltration into the fine layer and semi-infinite layers of soil. According to the Ross

(1990) model, water that accumulates at the interface between the MRL and the CBL only starts to flow down when suction reaches a critical value. Steenhuis et al. (1991) suggested that the critical suction value can be considered the water entry value (WEV) of the CBL, i.e. ψ_{WEV}^{CBL}. This parameter corresponds to the suction value at which the downward flow into the CBL (q_d) becomes equal to the seepage flow rate (q). Various studies have shown that the critical suction value definition suggested by Steenhuis et al. (1991) is more widely retained (Walter et al., 2000; Bussière et al., 2002; Nakafusa et al., 2012).

Based on the Ross (1990) model, the critical suction value is the suction at which the *k-fcts* of the MRL and CBL intersect. According to this analytical solution, the fine-grained material drains all the water down to the point where the critical suction value is attained. Abdolahzadeh et al. (2011b; 2011a), Parent and Cabral (2006), among others, presented evidence – based on field data and numerical simulations - that the downward flow into the CBL occurs gradually, often in a sigmoidal manner with distance. Considering this, Parent and Cabral (2006) developed a methodology based on the Ross (1990) model and proposed an empirical equation to quantify seepage flow into the CBL, taking into consideration a progressive downward flow into the coarse-grained material.

2.2.2 Numerical simulations

Numerical modeling of the Saint-Tite-des-Caps CCBE was performed in two distinct steps. In the first, the hydrological behaviour of the first two layers was investigated using Visual HELP (v. 2.2.03; Schlumberger Water Services), which considers the climate-dependent processes of precipitation, evapotranspiration and runoff. Visual HELP simulated the annual percolation rates reaching the top of the sand/gravel capillary barrier. In the second step, the unsaturated flow through the CCBE was simulated using SEEP/W (v. 2007; Geo-Slope Int. Ltd.). The simulated annual percolation rates obtained by Visual HELP were introduced in SEEP/W as an upper hydraulic boundary condition, for transient numerical simulations. For the steady state numerical simulation, the percolation rate value was fixed at 1 x 10^{-8} m/s, i.e. the k_{sat} of DBP.

2.2.3 Seepage flow rate reaching the capillary barrier: role of the seepage control layer

Abdolahzadeh et al. (2011a) analyzed field data from Saint-Tite-des-Caps experimental CCBE and found that the DBP layer diverts water laterally over a very short distance (less than 2.6 m), remaining saturated most of the time and along almost the entire length of the CCBE. Consequently, the DBP layer controls the amount of seepage reaching the sand/gravel capillary barrier. In order to evaluate this amount of seepage, the software Visual Help was used. Climatic data was obtained using a weather station (Vantage Pro; Davis Instruments) and was completed using the Visual HELP database (data from Quebec City). The main input data for the Visual HELP simulations are summarized in Table 2. A 5% slope was assigned to the model. The field capacity and wilting point moisture content input parameters, which are used to define moisture storage and unsaturated hydraulic conductivity, were obtained using the WRC. In all unsaturated layers, the initial moisture content was assumed equal to the wilting point value (Webb, 1997). Based on the results obtained from the Visual HELP simulations, the median year was adopted as typical year.

Table 2: Summary of HELP simulations input.

2.2.4 Geometry and boundary conditions of the capillary barrier model

Only the capillary barrier system consisting of sand and gravel that superimposes a layer of typical municipal solid waste was modelled in the present study. Given the fact that the DBP remained saturated at its base, a seepage boundary condition at the top of the sand layer was considered. The geometry and dimensions for the slightly inclined capillary barrier modelled herein are illustrated in Figure 2. The arbitrary thickness of the waste layer (0.5 m) was of little importance in the final results, given the coarse nature of this layer; i.e. the waste was not able to transmit any significant suction to the gravel layer, given the simulated seepage flow rate. The mesh density was adapted to improve the solution accuracy in critical zones, particularly at the sand-gravel interface (Chapuis, 2012). As it can be observed in Figure 2, various mesh densities were adopted. The vertical thickness of the elements near the sand-gravel interface and waste layer were 0.09 m and 0.25 m respectively. The horizontal length of the elements was similar throughout the model. A zero seepage horizontal flow was adopted at the upstream vertical boundary, which corresponds to the reality of the field experiment. A rectangular form was considered because it helped to achieve numerical stability. To avoid boundary effects on the right side of the model, the toe of the capillary barrier model was extended up to 200.0 m horizontally (Figure 2).

Three types of boundary conditions were used to simulate the Saint-Tite-des-Caps CCBE and are illustrated in Figure 2. At the downstream end of the model, two drains were located in the sand and gravel layers. These drainage outlets were simulated by applying a unit hydraulic gradient boundary. The physical meaning of this boundary condition was that the seepage flow rate that passed through the drainage outlet boundary at a given suction value was equal to the coefficient of permeability of the soil corresponding to that suction value (Tami et al., 2004). The water table was placed at the base of the waste layer, at a depth of 110 cm from the ground surface layer. A zero pressure boundary condition was imposed, representing the worst case (in fact, virtually impossible) scenario. It is assumed that maximum suction the wastes can transmit to the CBL is low enough so that the suction at the CBL-MRL interface is not affected by it. Accordingly, the shape of the WRC of the wastes does not affect the behaviour of the capillary barrier.

For the transient analysis, the initial pressure head at each node was obtained from the steady state simulation. The behaviour of the capillary barrier model was analyzed using wet initial conditions. This was considered as the worst condition, insofar as the capillary barrier model had a low storage capacity.

Figure 2: Basic model, geometry, dimensions, and boundary conditions of the Saint-Tite-des-Caps CCBE.

3 Results

3.1 Potential seepage flow rates

Lysimeters were installed in the sand layer to monitor the maximum amounts of water entering the sand/gravel capillary barrier for several years. A verification of their functionality was performed by Abdolahzadeh et al. (2011b), who concluded that, except for short periods of time, the lysimeters performed properly, i.e. suctions were equal to zero at the base and, at the top, their values were the same inside and immediately on the outside; in other words, there were no differences in total heads that could cause deviation or concentration of flow. As can be seen in Figure 3, field observations clearly indicated that the maximum seepage flow rate throughout 2006 (adopted year) did not exceed 1.0 x 10^{-8} m/s, i.e. the k_{sat} of DBP.

Figure 3: Evolution of seepage flow rates reaching the top of the sand/gravel capillary barrier by lysimeters installed in the sand layer at the Saint-Tite-des-Caps experimental CCBE, for year 2006 (adapted from Abdolahzadeh et al., 2008).

The results of the Visual HELP simulations are presented in Figure 4 for a typical simulated year. Seepage rate values equal to 1.9 x 10^{-8} m/s were sometimes obtained by the modeling process. Since they were not corroborated by field observations (Figure 3), seepage values greater than 1.0 x 10^{-8} m/s were set to 1.0 x 10^{-8} m/s. The seepage flow rates adopted as the upper boundary condition for the unsaturated flow simulations under transient state are indicated in Figure 4.

Figure 4: Visual HELP modeling results of the seepage flow rates through the DBP layer during a typical year.

3.2 Unsaturated flow simulations to determine DL

One of the goals of the numerical simulations was to estimate the approximate location of the diversion length along the sand/gravel capillary barrier. For practical purposes, instead of a region, the DL is associated herein with a precise distance from the top of the slope. The DL is located where the suction along the sand/gravel interface reaches the critical suction value ψ_{WEV} of the CBL (Steenhuis et al., 1991). From this location downslope, the suction at the interface tended to stabilize. In the present study, the diversion length was evaluated using 5 different approaches: 1) field data gathered from the Saint-Tite-des-Caps experimental CCBE; 2) a steady state numerical simulation; 3) a transient-state numerical simulation; 4) the Ross (1990) analytical model; and 5) the Parent and Cabral (2006) analytical model.

During the spring and summer of 2006, the DL at the Saint-Tite-des-Caps experimental CCBE was evaluated based on lysimeter, tensiometer and water content data. According to Abdolahzadeh et al. (2011b), the DL was located between 23.0 and 29.0 m (Figure 5). As observed by Abdolahzadeh et al. (2011a), suction values did stabilize downslope from the approximate DL region.

The seepage flow rates obtained from the transient and steady state analyses are also presented in Figure 5. It can be observed that when the flow rate value falls below 1.0 x 10^{-8} m/s, the DL given by the transient analysis increased accordingly. The lowest DL value obtained from the transient analysis was equal to the value obtained from the steady state analysis (DL = 19.0 m).

For the sake of comparison, the DL obtained using the Ross (1990) and Parent and Cabral (2006) models are also included in Figure 5. The Parent and Cabral (2006) model, with a DL=20.0 m, compared very well with the steady state DL, while the Ross (1990) model gave a very conservative DL value equal to 16.0 m. The very conservative nature of the DL by the Ross model results in part from the fact that this model is based on an "all-or-nothing" type of approach when it comes to determining the transfer capacity of the MRL and the diversion length.

In concluding, the lowest value of DL from the transient state analysis was equal to the DL obtained by modeling the CCBE under steady state and this value was quite close to what was actually observed in the field for the typical year analyzed. It is therefore tempting to conclude that steady state analyses could be a practical and effective choice for the design of CCBEs. Indeed, this can be the case under the following circumstances: when a CCBE is designed to minimize water infiltration and when a low permeability layer is installed above the MRL as a means to control the maximum seepage reaching it. Therefore, the maximum seepage flow reaching the MRL is equal to the k_{sat} of the seepage control layer. Zhang et al. (2004) observed that in order to maintain negative pore-water pressure values in a slope, it is important to reduce the infiltration flux through the use of a suitable type of cover system at the ground surface. Lim et al. (1996) carried out a field instrumentation program to monitor negative pore-water pressure values in residual soil slopes in Singapore that were protected by different types of surface covers. The changes in matric suction due to changes in ground surface moisture flux were found to be least significant under a canvas-covered slope and most significant in a bare slope. Several relatively impermeable surface covers can be adopted.

Figure 5: Evolution of the diversion length, as a function of the seepage flow rate (modified Visual HELP results, indicated as "adopted"; see Figure 4) and evolution of DL obtained by transient and, steady state analysis, as well as by using the Parent and Cabral (2006) and Ross (1990) models.

The level of confidence associated with the DL values obtained is intimately related to the level of confidence associated with the properties of the materials, the boundary conditions and initial conditions imposed on the model. It is therefore noteworthy that the DL obtained perfectly corroborates what was obtained by Abdolazadeh et al. (2011a) using lysimeter and tensiometer data. The accurateness of the material's properties was assessed by Abdolahzadeh et al. (2011b).

4 Conclusion

The design of CCBE is complex due to its transient behaviour, and several studies conclude that numerical simulations under transient states may better define the response of CCBE than those obtained from steady-state numerical or analytical solutions. Nevertheless, steady state solutions (numerical or analytical), associated with simplified assumptions and combined with particular boundary conditions, may allow engineers to make reasonable predictions using simple tools, thereby circumventing the difficulties and time involved to model a system under transient state.

The most important result of the research reported in this paper is that the DL obtained under steady state coincided with the worst-case scenario (in terms of diversion length) predicted by transient analysis, for the particular conditions of the Saint-Tite-des-Caps experimental CCBE. And it is relevant to note that the predicted DL was confirmed by field data. The present study concluded that steady state numerical analysis or an analytical solution such as Parent and Cabral (2006) predicts a conservative diversion length and, therefore, it is possible to use them during the preliminary design phase of a cover system that controls seepage into the waste mass.

Acknowledgements

Funding for this study was provided by Cascades Inc. and the Natural Sciences and Engineering Research Council (NSERC) (Canada) under the University–Industry Partnership grant number CRD 192179 and by NSERC under the second author's Discovery Grant. The authors also acknowledge help provided by Jean-Guy Lemelin, in the design of the experimental cells, installation of the measuring system and actual testing.

References

Abdolahzadeh, A.M., Lacroix Vachon, B. and Cabral, A.R. (2008). Hydraulic barrier and its impact on the performance of cover with double capillary barrier effect *In 61st Canadian Geotechnical Conference*. Edmonton. 21-24 Sept., CD-Rom.

Abdolahzadeh, A.M., Vachon, B.L. and Cabral, A.R. (2011a). Evaluation of the effectiveness of a cover with capillary barrier effect to control percolation into a waste disposal facility. *Canadian Geotechnical Journal*, **48**(7), 996-1009.

Abdolahzadeh, A.M., Vachon, B.L. and Cabral, A.R. (2011b). Assessment of the design of an experimental cover with capillary barrier effect using 4 years of field data. *Geotechnical and Geological Engineering*, **29**(5), 783-802.

Aubertin, M., Cifuentes, E., Apithy, S.A., Bussière, B., Molson, J. and Chapuis, R.P. (2009). Analyses of water diversion along inclined covers with capillary barrier effects. *Canadian Geotechnical Journal*, **46**(10), 1146-1164.

Aubertin, M., Cifuentes, E., Martin, V., Apithy, S., Bussiere, B., Molson, J., Chapuis, R.P. and Maqsoud, A. (2006). An investigation of factors that influence the water diversion capacity of inclined covers with capillary barrier effects. Carefree, AZ, United States, Geotechnical Special Publication 147, American Society of Civil Engineers, Reston, VA 20191-4400, United States, 613-624.

Barth, C. and Wohnlich, S. (1999). Proof of effectiveness of a capillary barrier as surface sealing of sanitary landfill. *In 7th International Waste Management and Landfill Symposium*. *Edited by* R. Cossu, R. Stegman, and T.H. Christensen. Sant Margarita di Pula, Italy, 389-392.

Bédard, D. (2005). Effet du fluage à long terme des sous-produits de désencrage dû à la perte de masse et son effet sur la compression et la conductivité hydraulique. M.Sc.A Thesis, Université de Sherbrooke, Sherbrooke, 166 p.

Brooks, R.H. and Corey, A.T. (1964). Hydraulic properties of porous media. *Hydrology paper no. 3, Colorado State University, Fort Collins, Colorado*.

Burnotte, F., Lefebvre, G., Cabral, A., Audet, C. and Veilleux, A. (2000). Use of deinking residues for the final cover of a MSW landfill. *In 53rd Canadian Geotechnical Conference*. Montreal. October 15-18, 2000, Vol. 1, 585-591.

Bussière, B., Aubertin, M. and Chapuis, R.P. (2002). A laboratory set up to evaluate the hydraulic behavior of inclined capillary barriers. *In International Conference on Physical Modelling in Geotechnics*. *Edited by* R. Phillips, P.J. Guo, and R. Popescu. St. John's, Newfoundland. July 2002, 391-396.

Bussière, B., Apithy, S., Aubertin, M. and Chapuis, R.P. (2003). Diversion capacity of sloping covers with capillary barrier effect. *In* 56th Annual Canadian Geotechnical Conf., 4th Joint IAH-CNC and CGS Groundwater Specialty Conf. & 2003 NAGS Conference, Winnipeg, Canada, p. 8,

Cabral, A.R., Planchet, L., Marinho, F.A. and Lefebvre, G. (2004). Determination of the soil water characteristic curve of highly compressible materials: case study of pulp and paper by-product. *Geot. Testing Journal*, **27**(2), 154-162.

Chapuis, R.P. (2004). Predicting the saturated hydraulic conductivity of sand and gravel using effective diameter and void ratio. *Canadian Geotechnical Journal*, **41**(5), 787-795.

Chapuis, R.P. (2012). Influence of element size in numerical studies of seepage: unsaturated zones, transient conditions. *Geotechnical News*, BiTech, Dec., 34-37 p.

Fredlund, D.G. and Xing, A.Q. (1994). Equations for the soil-water characteristic curve. *Canadian Geotechnical Journal*, **31**(4), 521-532.

Geo-Slope (2004). SEEP/W User's Manual,

Giurgea, V.I., Hötzl, H. and Breh, W. (2003). Studies on the long-term performance of an alternative surface-sealing system with underlying capillary barrier *In Sardinia 2003 - 9th International Landfill Symposium*. *Edited by* R. Cossu and R. Stegmann. St-Margarita di Pula, Italy. Oct. 2003, CISA, Paper 307 - CD-Rom.

Hazen, A. (1911). Discussion of "Dams on Sand Foundations" from A.C. Koening. *ASCE*, **73**.

Hupe, K., Heyer, K.-U., Becker, J.F., Traore, O., Noetzel, S. and Stegmann, R. (2003). Investigations of alternative landfill surface sealing systems in test fields *In Sardinia 2003 - 9th International Landfill Symposium*. *Edited by* R. Cossu and R. Stegmann. St-Margarita di Pula, Italy. Oct. 2003, CISA, Paper 582 - CD-Rom.

Kämpf, M., Holfelder, T. and Montenegro, H. (2003). Identification and parameterization of flow processes in artificial capillary barriers. *Water Resources Research*, **39**(10), 21-29.

Khire, M.V., Benson, C.H. and Bosscher, P.J. (2000). Capillary barriers: Design variables and water balance. *Journal of Geotechnical and Geoenvironmental Engineering*, **126**(8), 695-708.

Lacroix Vachon, B. (2008). Les écoulements dans les milieux non saturés et leurs applications aux couvertures avec effet de barrière capillaire installées dans un site d'enfouissement sanitaire Dissertation Thesis, Université de Sherbrooke, Sherbrooke, 138 p.

Lacroix Vachon, B., El-Ghabi, B. and Cabral, A.R. (2007). Évaluation préliminaire de l'efficacité du recouvrement avec double effet de barrière capillaire installé au site de St-

Tite-des-Caps, Qc. *In 60^{th} Canadian Geotechnical Conference*. Ottawa. 21-24 Oct., Vol. CD-Rom.

Lim, T.T., Rahardjo, H., Chang, M.F. and Fredlund, D.G. (1996). Effect of rainfall on matric suctions in a residual soil slope. *Canadian Geotechnical Journal*, **33**(4), 618-628.

Maqsoud, A., Bussière, B. and Aubertin, M. (2004). Hysteresis effects on the water retention curve: a comparison between laboratory results and predictive models. *In 57^{th} Canadian Geotechnical Conference and the 5^{th} Joint CGS-IAH Conference*. Quebec City, Canada, CGS, Vol. Session 3A, 8-15.

Morel-Seytoux, H.J. (1994). Steady-state effectiveness of a capillary barrier on a sloping interface. *In 14th Hydrology Days*. *Edited by* H.J. Morel-Seytoux. Atherton, CA, Hydrology Days Publications, 335-346.

Morris, C.E. and Stormont, J.C. (1998). Evaluation of numerical simulations of capillary barrier field tests. *Geotechnical and Geological Engineering*, **16**, 201-213.

Morris, C.E. and Stormont, J.C. (1999). Parametric study of unsaturated drainage layers in a capillary barrier. *Journal of Geotechnical & Geoenvironmental Engineering*, **125**(12), 1057-1065.

Mualem, Y. (1976). A new model for predicting the hydraulic conductivity of unsaturated porous media. *Water Resources Research*, **12**, 513-522.

Nakafusa, S., Kobayashi, K., Morii, T. and Takeshita, Y. (2012). Estimation of water diversion provided by capillary barrier of soils. *In 5^{th} Asia-Pacific Conference on Unsaturated Soils 2012*. Pattaya, Thailand. Feb. 29 - March 2, 2012, Geotechnical Engineering Research and Development Center, Vol. 2, 643-647.

Parent, S.-É. (2006). Aspects hydrauliques et géotechniques de la conception de barrières capillaires incluant des matériaux recyclés hautement compressibles. Dissertation/Thesis Thesis, Université de Sherbrooke, Sherbrooke, 114 p.

Parent, S.-É. and Cabral, A.R. (2006). Design of inclined covers with capillary barrier effect. *Geotechnical and Geological Engineering Journal*, **24**, 689-710.

Parent, S.-É., Cabral, A.R. and Zornberg, J.G. (2007). Water retention curves and hydraulic conductivity functions of highly compressible materials. *Canadian Geotechnical Journal*, **44**(10), 1200-1214.

Parent, S.-É., Cabral, A.R., Dell' Avanzi, E. and Zornberg, J.G. (2004). Determination of the hydraulic conductivity function of a highly compressible material based on tests with saturated samples. *Geot. Testing Journal*, **27**(6), 1-5.

Planchet, L. (2001). Utilisation des résidus de désencrage comme barrière capillaire et évapotranspirative (ET) pour les parcs à résidus miniers producteurs de DMA Thesis, Université de Sherbrooke, Sherbrooke, 114 p.

Ross, B. (1990). Diversion capacity of capillary barriers. *Water Resources Research*, **26**(10), 2625-2629.

Steenhuis, T.S., Parlange, J.Y. and Kung, K.J.S. (1991). Comment on 'the diversion capacity of capillary barriers' by Benjamin Ross (paper 91WR01366). *Water Resources Research*, **27**(8), 2155.

Stormont, J.C. (1996). The effectiveness of two capillary barriers on a 10% slope. *Geotechnical and Geological Engineering Journal*, **14**, 243-267.

Tami, D., Rahardjo, H., Leong, E.C. and Fredlund, D.G. (2004). Design and laboratory verification of a physical model of sloping capillary barrier. *Canadian Geotechnical Journal*, **41**, 814 - 830.

van Genuchten, M.T. (1980). A closed-form equation for predicting the hydraulic conductivity of unsaturated soils. *Soil Science Society of America Journal*, **44**, 892-898.

van Genuchten, M.T., Leij, F.J. and Yates, S.R. (1991). The RETC code for quantifying the hydraulic functions of unsaturated soils. In: (eds), Report EPA/600/2-91/065, U.S. Department of Agriculture, Agriculture Research Service p.

von Der Hude, N., Melchior, S. and Möckel, S. (1999). Construction of a capillary barrier in the cover of the Breinermoor landfill. *In Seventh International Waste Management and Landfill Symposium*. *Edited by* T.H. Christensen, R. Cossu, and R. Stegmann. Sta Margarita di Pula, Italy, CISA, 393-402.

Walter, M.T., Kim, J.S., Steenhuis, T.S., Parlange, J.Y., Heilig, A., Braddock, R.D., Selker, J.S. and Boll, J. (2000). Funneled flow mechanisms in a sloping layered soil: Laboratory investigation. *Water Resources Research*, **36**(4), 841-849.

Wawra, B. and Holfelder, T. (2003). Development of a landfill cover with capillary barrier for methane oxidation - the capillary barrier as gas distribution layer. *In 9th Int. Waste Mgmt and Landfill Symp.* Italy. October 6-10, 2003, Paper 348.

Webb, S.W. (1997). Generalization of Ross Tilted Capillary Barrier Diversion Formula for Different Two-Phase Characteristic Curves. *Water Resources Research*, **33**(8), 1855-1859.

Yanful, E.K., Mousavi, M. and De Souza, L.P. (2006). A numerical study of soil cover performance. *Journal of Environmental Management*, **81**, 72–92.

Zhan, G., Mayer, A., McMullen, J. and Aubertin, M. (2001). Slope effect study on the capillary cover design for a spent leach pad. *In 8th International Conference Tailings and Mine Waste '01*. Colorado State University, Forth Collins, Co., Balkema, 179-187.

Zhang, L.L., Fredlund, D.G., Zhang, L.M. and Tang, W.H. (2004). Numerical study of soil conditions under which matric suction can be maintained. *Canadian Geotechnical Journal*, **41**, 569–582.

Zhang, Q., Werner, A., Aviyanto, R. and Hutson, J. (2009). Influence of soil moisture hysteresis on the functioning of capillary barriers. *Hydrological Processes*, **23**, 1369-1375.

Tables

Table **1**: Hydraulic properties of the materials used in numerical simulations of the Saint-Tite-des-Caps experimental CCBE.

Parameters	DBP	Sand	Gravel	Waste
WRC's model	FX [1]	vG [2]	vG [2]	vG [2]
α [3] [4]	45.5	0.472	1.953	0.38
n [3]	1.42	6.32	4.20	1.47
m [3]	0.876	0.842	0.762	0.32
Cr (kPa) [5]	2000	n/a	n/a	n/a
θ_s (m^3/m^3)	0.77	0.33	0.35	0.30
θ_r (m^3/m^3)	n/a	0.05	0.07	0.01
k_{sat} (m/s) [6]	$1x10^{-8}$	$1.5x10^{-4}$	$1.5x10^{-3}$	$1.0x10^{-5}$
ψ_{AEV} (kPa) [7]	~ 14	~ 1.4	~ 0.4	~ 2.6
ψ_{WEV} (kPa) [8]	---	~ 3.5	1.7 [9]	~ 200

Note:

(1) FX: Fredlund and Xing (1994);

(2) vG: van Genuchten (1980);

(3) α, n, m are van Genuchten (1980) parameters;

(4) 1/kPa for van Genuchten model, kPa for Fredlund and Xing model;

(5) Cr: in Fredlund and Xing (1994) model, this parameter is a constant derived from the residual suction, i.e. the tendency to the null water content;

(6) k_{sat} is saturated hydraulic conductivity;

(7) ψ_{AEV} is the suction value at air entry value;

(8) ψ_{WEV} is the suction value at water entry value;

(9) Rounded value.

Table **2**: Summary of HELP simulations input.

Layer	Thickness (m)	Properties	HELP layer type	Total porosity (vol/vol)	Field capacity (vol/vol)	Wilting point (vol/vol)	k_{sat} (m/s)	Subsurface inflow (mm/year)
Loamy fine sand	0.6	Top soil (protection layer)	Vertical percolation	0.453	0.19	0.085	7.2×10^{-6}	0
DBP	0.6	Barrier soil (seepage control layer)	Barrier soil liner	0.775	0.71	0.231	1.0×10^{-8}	0

Figures

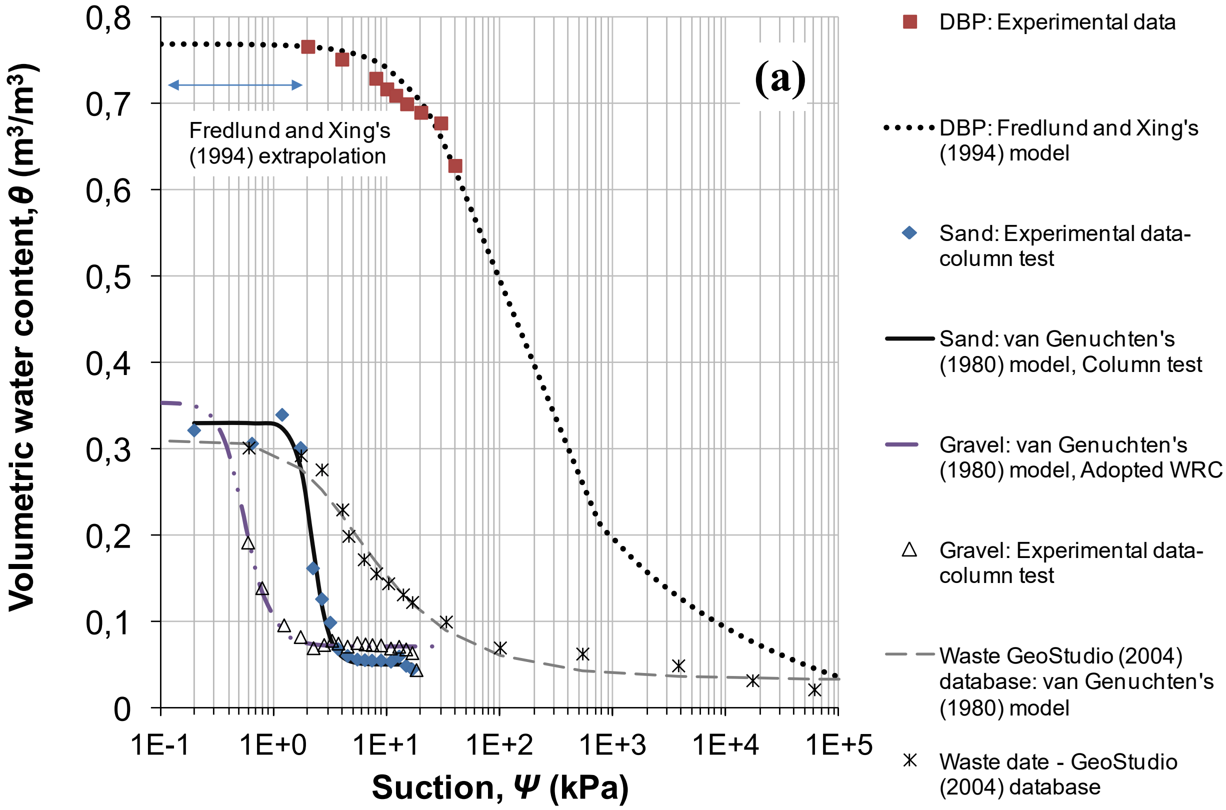

0,8
0,7
0,6
0,5
0,4
0,3
0,2
0,1
0
Volumetric water content, θ (m³/m³)
1E-1
1E+0
1E+1
1E+2
1E+3
1E+4
1E+5
Suction, Ψ (kPa)
(a)
Fredlund and Xing's (1994) extrapolation
DBP: Experimental data
DBP: Fredlund and Xing's (1994) model
Sand: Experimental data-column test
Sand: van Genuchten's (1980) model, Column test
Gravel: van Genuchten's (1980) model, Adopted WRC
Gravel: Experimental data-column test
Waste GeoStudio (2004) database: van Genuchten's (1980) model
Waste date - GeoStudio (2004) database

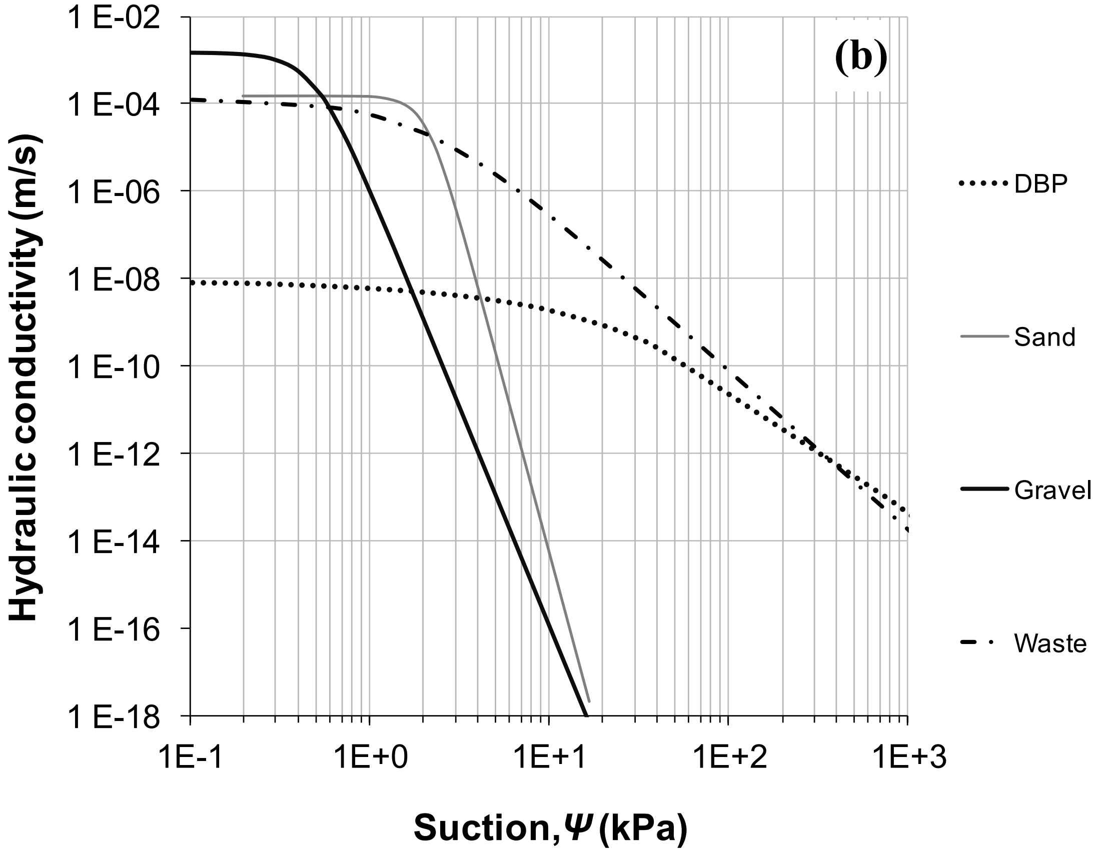

Figure 1: a) Water retention curve (WRC); and b) *k-fct* of the materials used in numerical simulations.

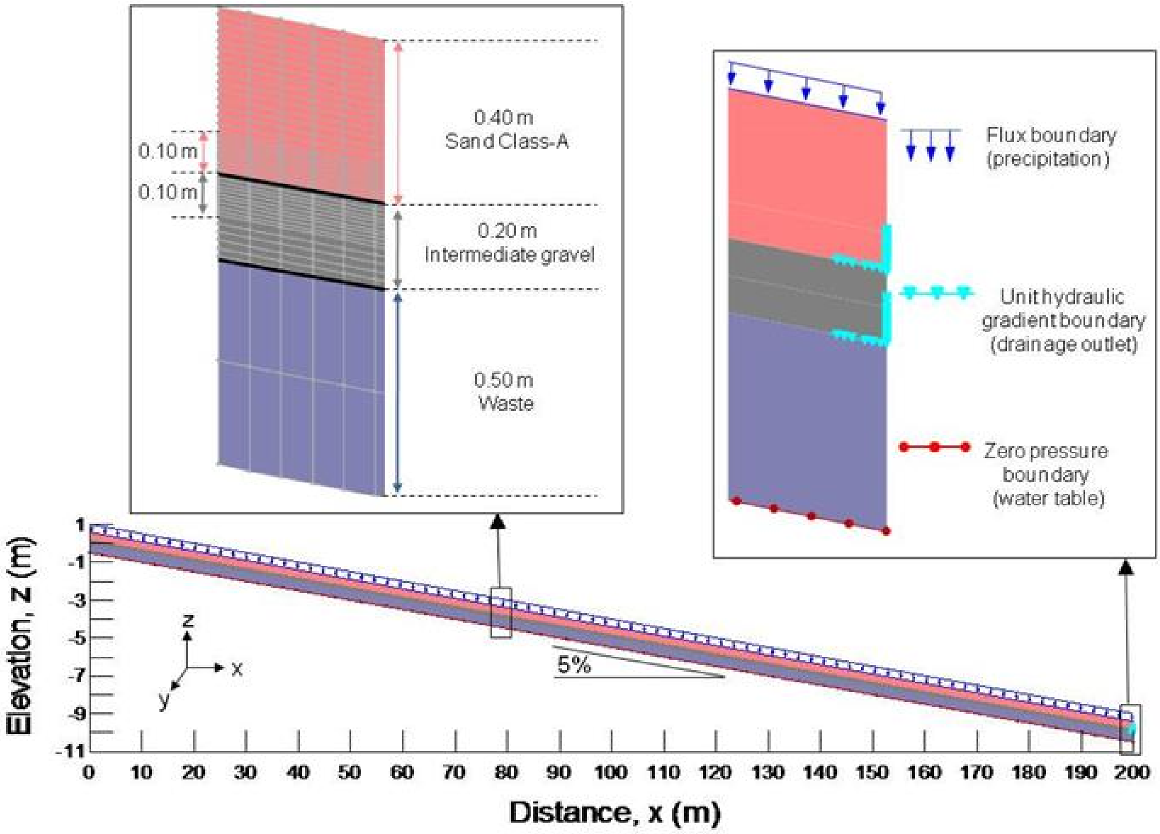

Figure 2: Basic model, geometry, dimensions, and boundary conditions of the Saint-Tite-des-Caps CCBE.

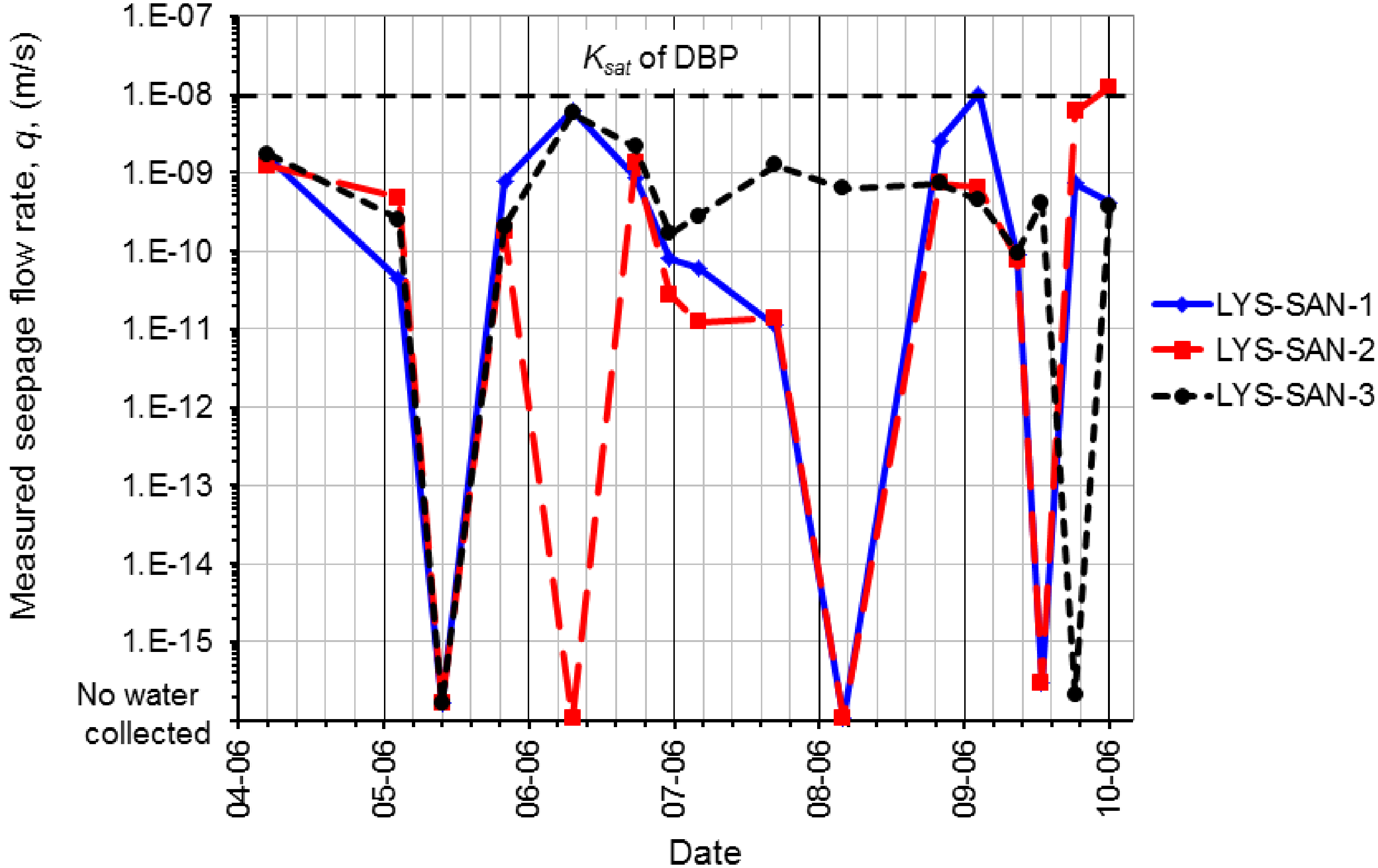

Figure 3: Evolution of seepage flow rates reaching the top of the sand/gravel capillary barrier by lysimeters installed in the sand layer at the Saint-Tite-des-Caps experimental CCBE, for year 2006 (adapted from Abdolahzadeh et al., 2008).

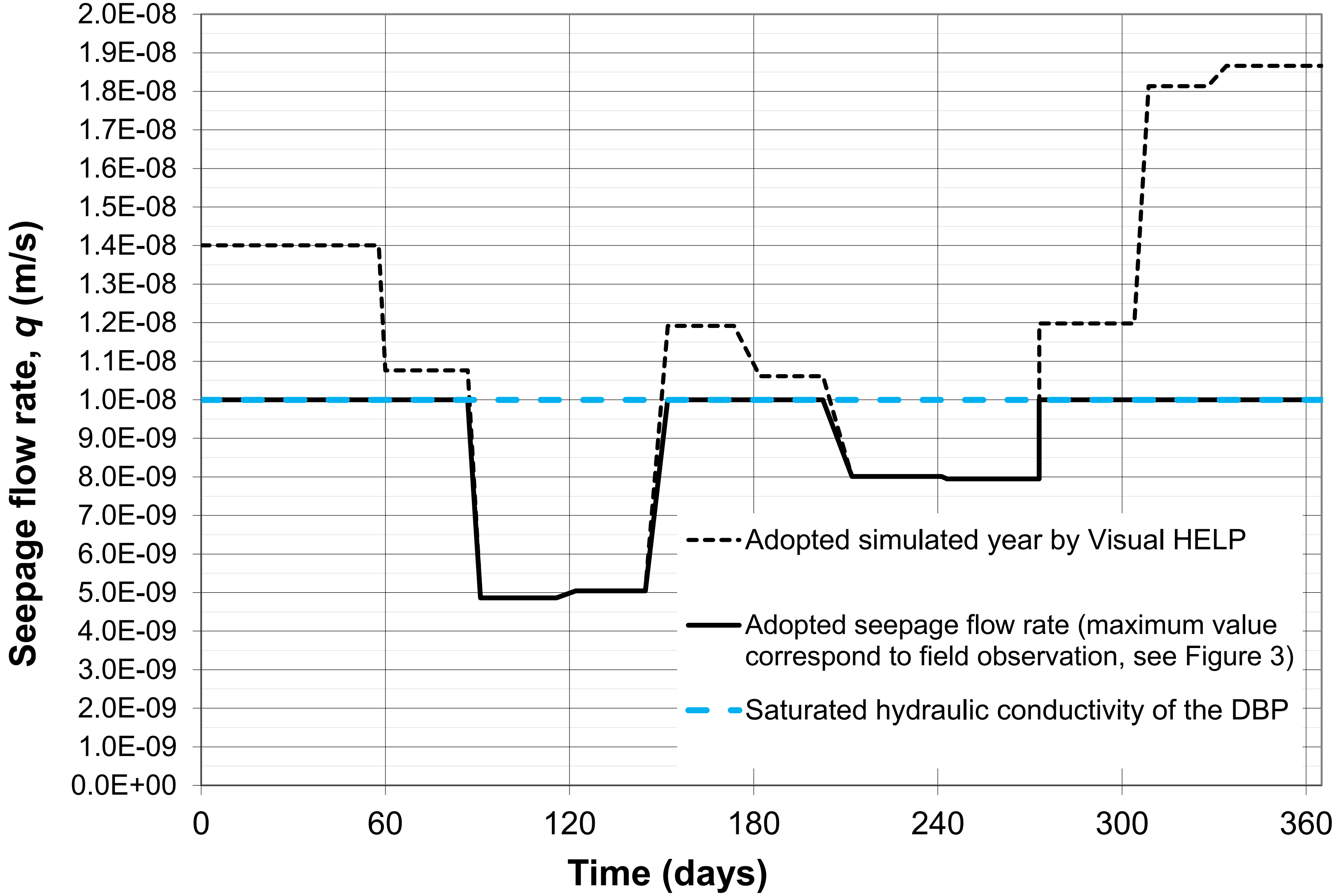

Figure 4: Visual HELP modeling results of the seepage flow rates through the DBP layer during a typical year.

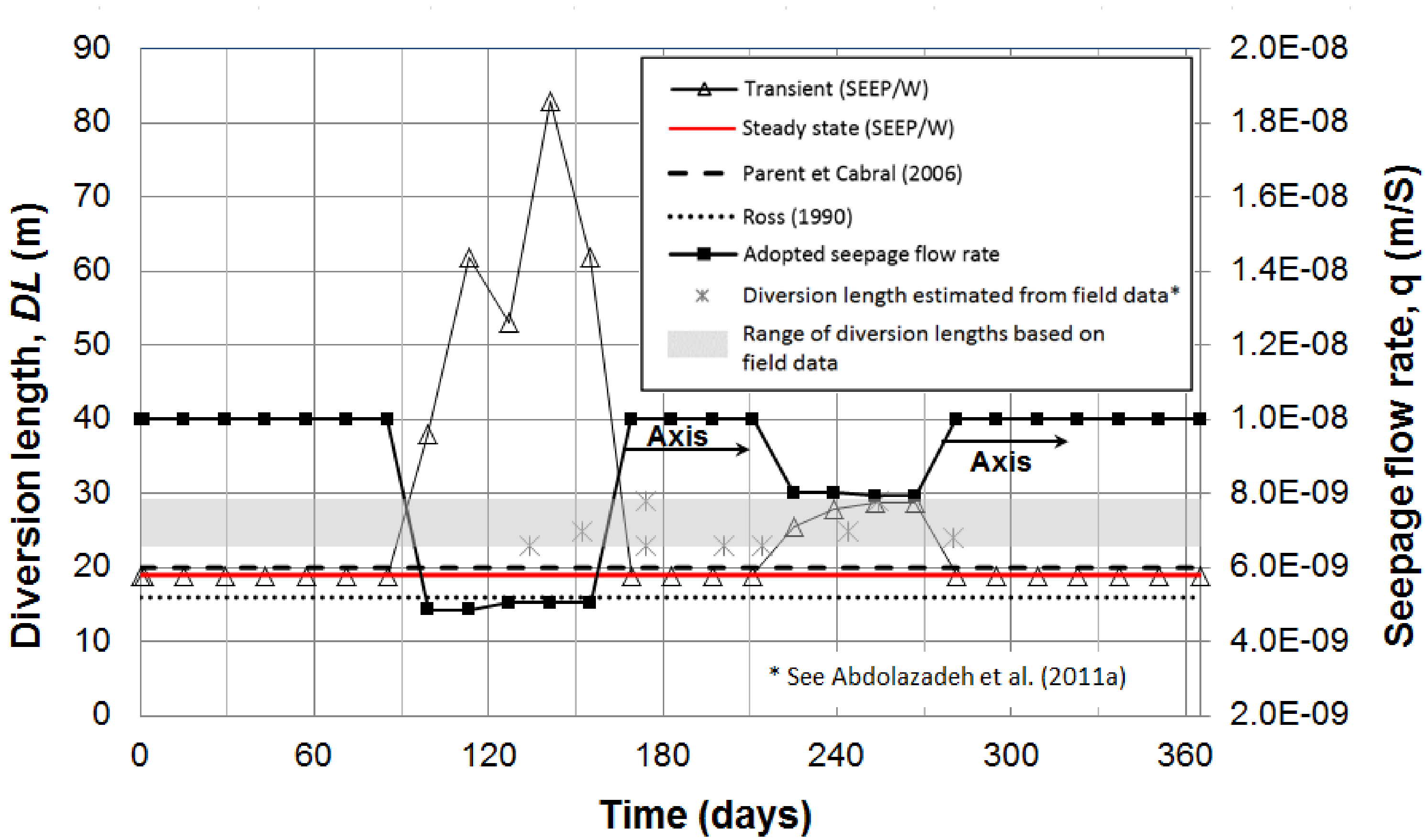

Figure 5: Evolution of the diversion length, as a function of the seepage flow rate (modified Visual HELP results, indicated as "adopted"; see Figure 4) and evolution of DL obtained by transient and, steady state analysis, as well as by using the Parent and Cabral (2006) and Ross (1990) models.